

Article

Determination of the Extent of the Rock Destruction Zones around a Gasification Channel on the Basis of Strength Tests of Sandstone and Claystone Samples Heated at High Temperatures up to 1200 °C and Exposed to Water

Krzysztof Skrzypkowski ^{1,*} , Krzysztof Zagórski ²  and Anna Zagórska ³

¹ Faculty of Civil Engineering and Resource Management, AGH University of Science and Technology, Mickiewicza 30 Av., 30-059 Kraków, Poland

² Faculty of Mechanical Engineering and Robotics, AGH University of Science and Technology, Mickiewicza 30 Av., 30-059 Kraków, Poland; zagkrzys@agh.edu.pl

³ Research Centre in Kraków, Institute of Geological Sciences, Polish Academy of Science, Senacka 1, 31-002 Kraków, Poland; a.zagorska@ingpan.krakow.pl

* Correspondence: skrzypko@agh.edu.pl; Tel.: +48-126-172-160



Citation: Skrzypkowski, K.; Zagórski, K.; Zagórska, A. Determination of the Extent of the Rock Destruction Zones around a Gasification Channel on the Basis of Strength Tests of Sandstone and Claystone Samples Heated at High Temperatures up to 1200 °C and Exposed to Water. *Energies* **2021**, *14*, 6464. <https://doi.org/10.3390/en14206464>

Academic Editors: Ján Kačur, Milan Durdán and Marek Laciak

Received: 6 September 2021

Accepted: 7 October 2021

Published: 9 October 2021

Publisher's Note: MDPI stays neutral with regard to jurisdictional claims in published maps and institutional affiliations.



Copyright: © 2021 by the authors. Licensee MDPI, Basel, Switzerland. This article is an open access article distributed under the terms and conditions of the Creative Commons Attribution (CC BY) license (<https://creativecommons.org/licenses/by/4.0/>).

Abstract: This article presents the results of laboratory tests regarding the influence of high temperatures on changes in the strength and structural parameters of rocks that are present in the immediate vicinity of a gasification channel. Sandstone and claystone samples were heated at 300 °C, 600 °C, 900 °C and 1200 °C. Additionally, the heated samples were placed in water for 24 h. The results of the laboratory tests were used in the numerical simulation using RS2 software. The main goal of modeling was to determine the extent of the rock destruction zone around the gasification channel for dry and wet rock masses. In the numerical simulations, three widths of the gasification channel and three ranges of high-temperature impact were modeled. On the basis of the obtained results, it was found that the extent of rock destruction, both in the roof and in the floor, is greater by several percent for a wet rock mass. For the first time, this research presents the effect of water on heated rock samples in terms of the underground coal gasification process. The results of laboratory tests and numerical simulations clearly indicate a reduction in strength, deformation and structural parameters for the temperature of 1200 °C.

Keywords: high temperature; strength and structural parameters of rocks after heating; destruction zone around gasified channel

1. Introduction

Underground coal gasification is a prospective method for obtaining useful minerals, in particular from deposits that are considered sub-balance. First of all, it is an environmentally friendly method due to the lack of waste generation on the surface [1] and a much smaller number of preparatory excavations [2]. Coal seams which are accessed using unprofitable opencast or underground methods are the subject of particular interest [3]. One of the criteria for underground mining is coal thickness. For example, in accordance with the Polish criteria for the balance of mineral deposits, the minimum thickness of hard coal in the seam together with interlayers up to 0.3 m thick should be at least 1 m for balance deposits and 0.6 m for sub-balance deposits [4]. Underground gasification encounters a number of obstacles resulting from changing geological and hydrogeological conditions [5]. As a result of high temperatures, the solubility of pollutants in water increases and the possibility of their migration to aquifers occurs. Hazardous inorganic pollutants include ammonia and cyanides [6]. During the process, numerous impurities in the form of aromatic organic compounds are formed, including: benzene, toluene, ethylbenzene, xylenes, phenols and polycyclic aromatic hydrocarbons. Additionally, significant amounts of heavy

metals may be released from coal and the ashes generated during gasification in volatilization processes, which are favored by the high temperature of the process and the presence of numerous chemical factors [7]. Rock minerals have specific thermal properties. Heat conduction through the minerals is partially absorbed as energy. The heat is absorbed differently by the mineral, depending on the direction of the heat flow in relation to the crystallographic axis. The pronounced directivity in heat conduction in many minerals is similar to the directivity in the refraction of light rays and the coefficient of linear thermal expansion. The thermal conductivity of rocks can be defined as the transfer of thermal energy by the disordered movement of particles from higher to lower temperatures [8]. Tian et al. [9] pointed out that high temperatures lead to micro-cracks and damage rock microstructures. Liu et al. [10] distinguished three stages of temperature propagation in the surrounding rock of a combustion cavity and stated that mechanical properties of coal and rock are determined by its extreme temperature. Perkins [11] indicated that the coal spalling process leads to cavity growth. Min et al. [12] found a relationship between pyrolysis temperature and pore fissures, ranging from rough and porous to relatively smooth. Feng et al. [13] and Deming et al. [14] stated that the gasification reaction occurs on the surface of micropores.

A gasifying agent (oxygen, oxygen together with water vapor, heated air or oxygen-enriched air) and gas can sometimes filter through rocks in an undesirable direction. It is also worth paying attention to the fact that as a result of high temperatures, the rocks surrounding a gasified coal seam change their porosity and permeability [15]. Yavuz et al. [16] found that for carbonate rocks, the bulk density decreased with increasing temperature. Chaki et al. [17] noticed that for granite rock samples, there was an increase in porosity in the temperature range from 500 °C to 600 °C, which is related to the increase in the number of fractures. Tian et al. [18] indicated that for sandstone, the thermal expansion of minerals changes with increasing temperature, which in turn contributes to a change in the microcrack network and the spread of structural damage to rocks. Małkowski et al. [19] found a relationship between high temperatures and the thermal conductivity factor, the value of which for sandstone, claystone and siltstone increase fourteen times at 1000 °C compared to 20 °C. In the gasification channel, oxidation, reduction and pyrolysis zones can be separated [20]. A characteristic feature of the underground gasification process is the fact that each of these reactions takes place at a temperature of several hundred degrees, and even exceeding 1000 °C [21]. Such high temperatures change the strength and post-critical parameters of rocks and rock mass and obviously change the stability conditions underground, which are necessary in the process of underground coal gasification [22]. Otto et al. [23] determined that parameters such as tensile strength, elastic modulus and the linear thermal expansion factor have a direct impact on changes in stresses and strains around the georeactor. Model studies confirm that impact of a range of high temperatures significantly exceeds the boundaries of the gasification channel [24]. In both laboratory [25] and industrial conditions [26], temperatures above 1000 °C may remain in the gasification channel for more than 36 h after ignition. Falsztinskij et al. [27], on the basis of model studies, determined that the maximum range of the temperature field was located above the fire channel; at the edge of the transition of the oxidation zone into the reduction zone with a temperature of 950–1200 °C, the following parameters were found: width of the transition zone, 0.74–1.5 m; height of temperature propagation, up to 9 m from the coal seam perpendicular to the rock stratification.

Despite the significant progress that has been made in both industrial and laboratory work on the underground coal gasification process, there is still little data on the behavior of rocks under the influence of high temperatures which were then exposed to water after this process. Therefore, this article presents laboratory tests regarding sandstone and claystone rock samples which were heated at 300 °C, 600 °C, 900 °C and 1200 °C. Additionally, after being heated, a new series of samples were immersed in water for 24 h and subjected to strength tests. The aim of the research was to compare the results with samples tested at

20 °C. The results of laboratory tests were used in numerical modeling, the aim of which was to determine the extent of the destruction zone around the gasification channel.

2. Preparation of Samples for Testing

Rock samples of sandstone and claystone were collected from the floor of the preparatory roadway in one of the mines of Jastrzębska Spółka Węglowa in Poland, which was closed due to the small thickness of hard coal deposits. The roadway was located at a depth of 900 m. The coal seam was located at a depth of 980 m. The average thickness of the seam in the area covered by the research was 0.4 m. Directly in the roof of the seam there was claystone with a thickness of 0.6 m, above which, sandstone with a thickness of 27 m was deposited. At the floor of the seam, there was a 0.5 m-thick claystone, below which, there was a 22 m-thick sandstone layer (Figure 1a). Rock cores with diameters of 48 mm were taken from the floor of the roadway (Figure 1b,c). The claystone was gray and dark gray in color and showed a solid and orderly structure. Sedimentary structures, parallel and diagonal layering were visible. In the case of texture, the grain skeleton was compact, with grain diameter varying from the very fine sand fraction to the aleurite fraction. The binder was porous and in terms of chemical composition, it was clay–silica. The mineral composition was mainly quartz, clay minerals in various proportions and mica. In turn, medium-grained sandstone was gray with a massive and ordered structure. Macroscopically, it was concise and uniform, without voids and cavities. In the sandstone, sedimentary structures and layering were visible, emphasized by a change in color and a variable grain diameter. The grain skeleton was compact. The sandstone binder was porous and siliceous. In terms of mineral composition, quartz dominated; moreover, there were traces of feldspar, mica and carbonaceous matter that formed streaks.

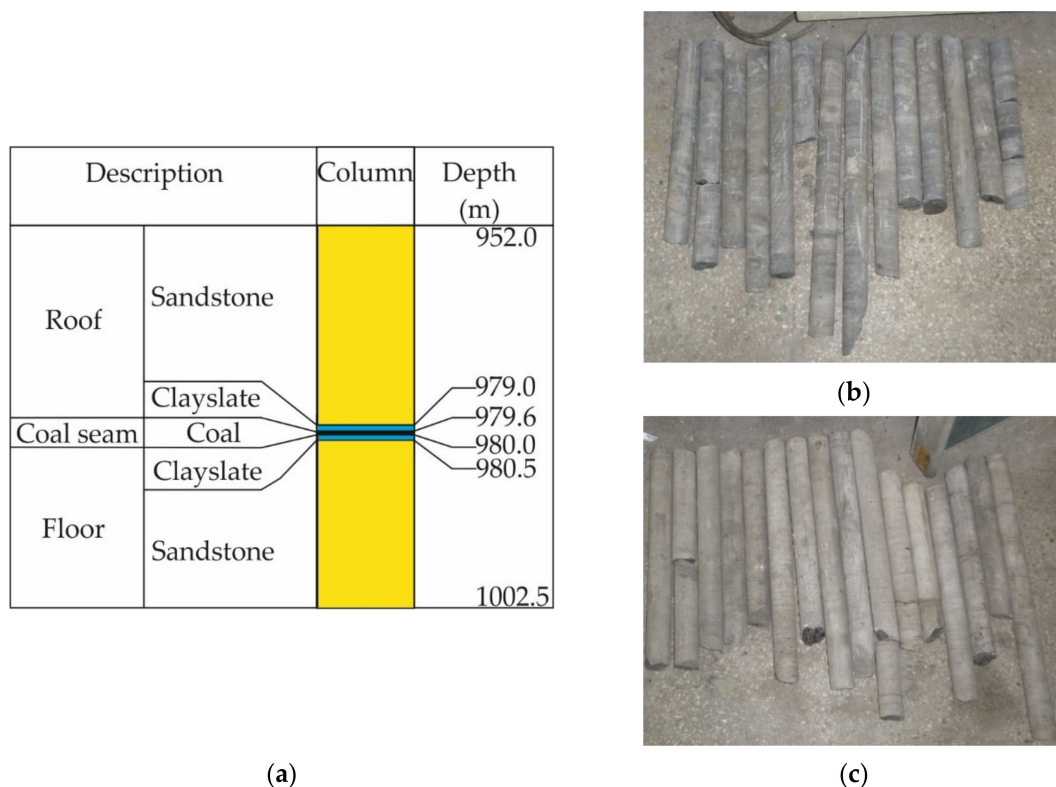


Figure 1. Place of sampling: (a) lithological profile of the immediate vicinity of the hard coal seam; (b) claystone cores; (c) sandstone cores.

The rock cores were cut into cylindrical samples with a height-to-diameter ratio of 2:1. The samples were prepared in such a way that it was possible to apply the load in the direction perpendicular to the stratification (Figure 2a,b). Laboratory tests were divided

into several stages. First, the tests were carried out at the temperature of 20 °C. Then, the samples were heated for 24 h at the temperatures of 300 °C, 600 °C, 900 °C and 1200 °C. A laboratory furnace with a maximum heating temperature of 1600 °C was used in the tests (Figure 2c). In the last stage of the tests, a new series of samples were heated at the same temperatures as before, and then the samples were immersed in water for 24 h. The samples were heated in the laboratory of the Faculty of Mechanical Engineering and Robotics, AGH University of Science and Technology in Krakow.



(a)



(c)



(b)

Figure 2. Preparation for tests: (a) regular samples of claystone; (b) regular samples of sandstone; (c) heating in a laboratory furnace.

Research on the influence of water on the strength and deformation parameters of rocks after heating took place due to the fact that the hard coal seam was classified as being a third-degree water hazard zone. On the basis of drilling and exploratory research in the mine, it was found that in the roof and floor of the deposit, there was an aquifer of the fissure and fissure-cavern type, not separated with a sufficient thickness and with a continuous insulating layer from the deposit. In addition, in the part of the rock mass where mining was planned to be carried out, there were water reservoirs containing water under pressure in relation to the floor of these seams.

3. Strength, Deformation and Structural Parameters of Sandstone and Claystone Heated at High Temperatures

Strength tests regarding sandstone and claystone heated at 300 °C, 600 °C, 900 °C and 1200 °C were carried out in a hydraulic press at the laboratory of the Faculty of Civil Engineering and Resource Management at the University of Science and Technology in Krakow. The load measurement was carried out using three strain gauge force sensors, while to determine the vertical deformation, a line encoder with a sampling frequency of 100 Hz was used. In order to determine the horizontal deformations, three electronic sensors were used and spaced 120° apart on the circumference of the sample. The load rate was 0.1 kN/s. After heating, the samples were tested at room temperature, about 20 °C. The load and deformation sensors were connected to the measuring amplifier, which in turn was connected to a computer on which the load–displacement characteristics were monitored on an ongoing basis. Young’s modulus was determined at the value of 20–80% of the breaking stress. The density of the samples was determined using the hydrostatic

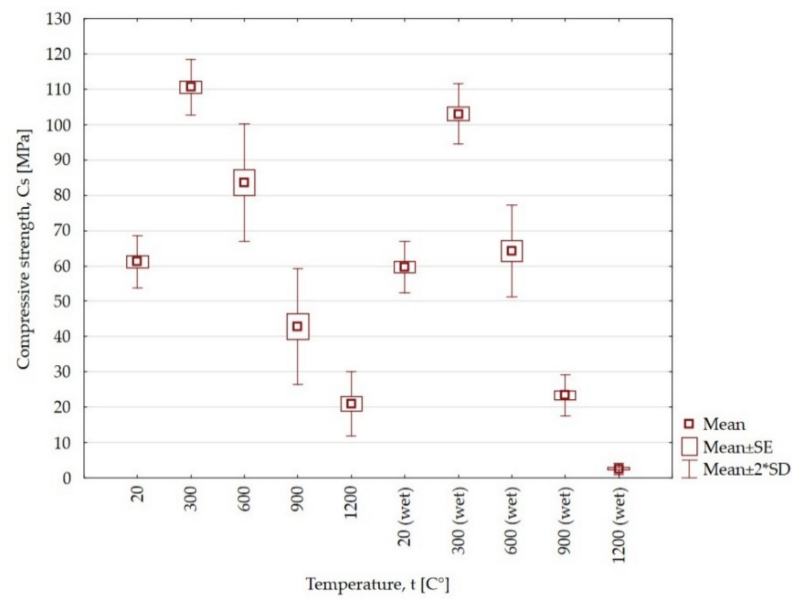
method [28] with the use of a WPS 210/C/1 laboratory balance. Additionally, for the temperatures of 300 °C, 600 °C, 900 °C and 1200 °C, the weight loss was determined. The samples were weighed on a WPT 2 laboratory balance. As a result of the temperatures of 600 °C, 900 °C and 1200 °C, the claystone samples lost their cohesion and divided into irregular pieces. Moreover, several samples were also damaged at the temperature of 300 °C (Figure 3). On the other hand, sandstone samples heated at 300 °C, 600 °C, 900 °C kept their form. Only at the temperature of 1200 °C did numerous cracks appear (Figure 4). The results of the compressive strength, tensile strength, Young's modulus, Poisson ratio, density and weight loss tests are shown in Figures 5–10.



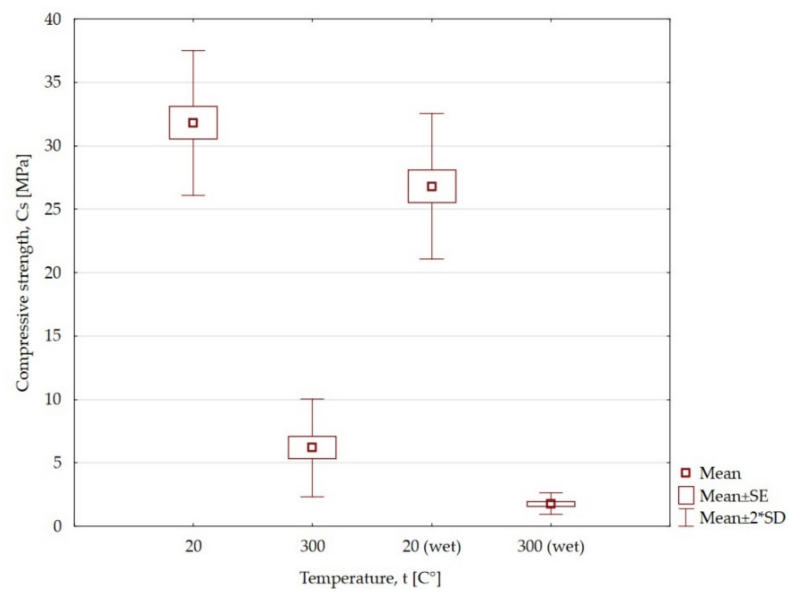
Figure 3. Claystone heated at high temperatures.



Figure 4. Sandstone heated at high temperatures.



(a)



(b)

Figure 5. The influence of high temperatures on changes in uniaxial compression strength of dry and wet samples: (a) sandstone; (b) claystone; SE—standard error; SD—standard deviation.

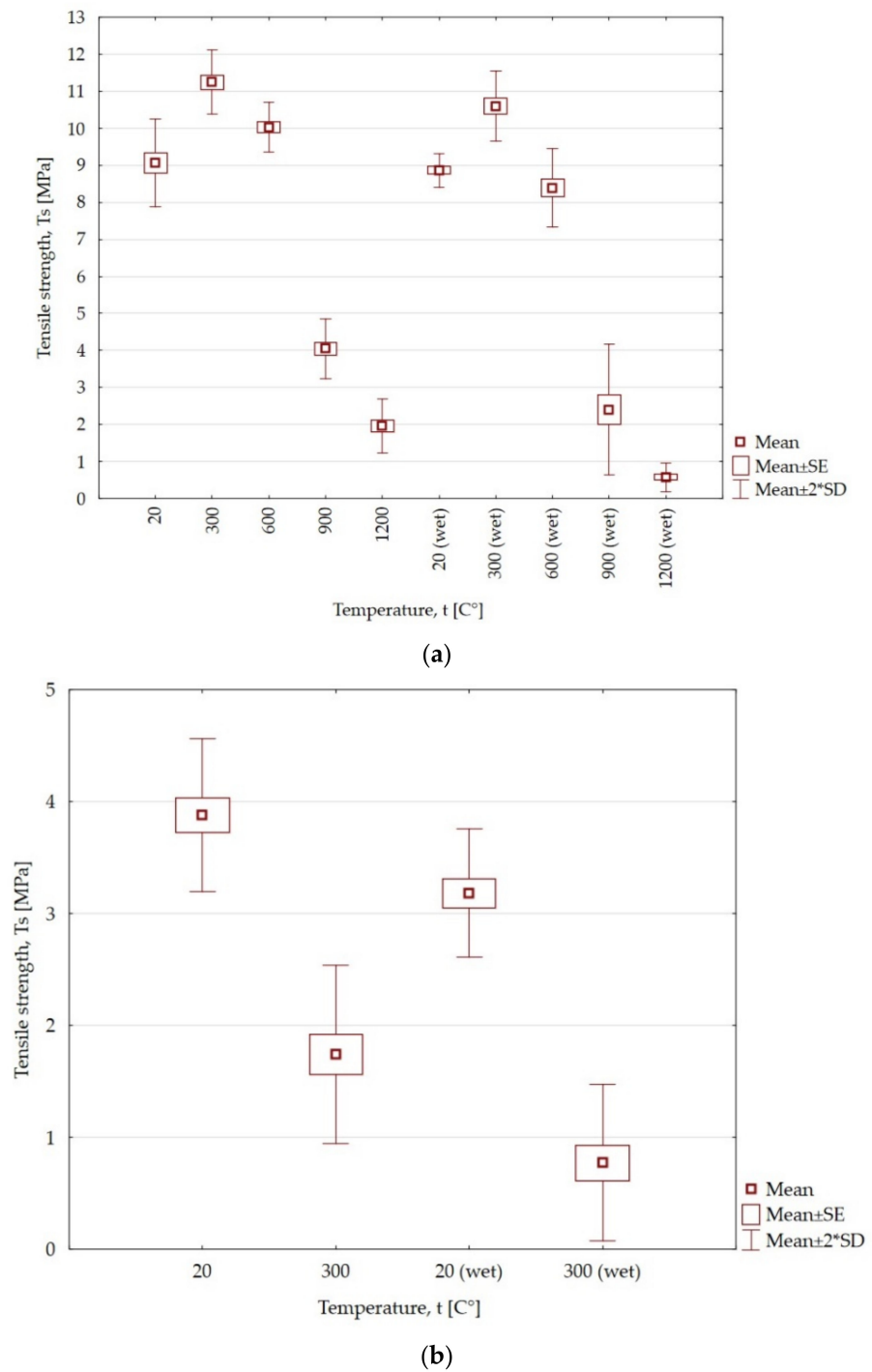
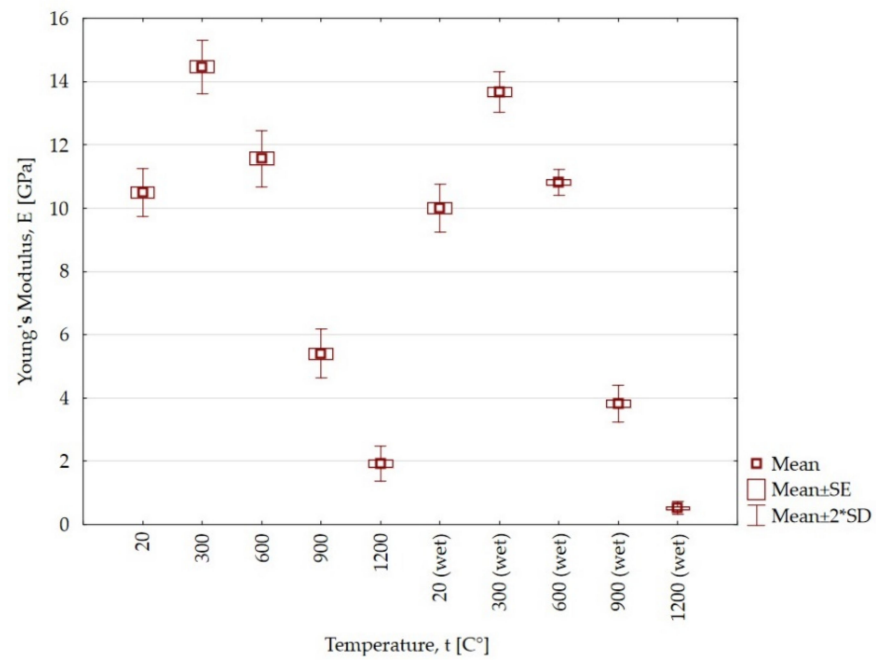
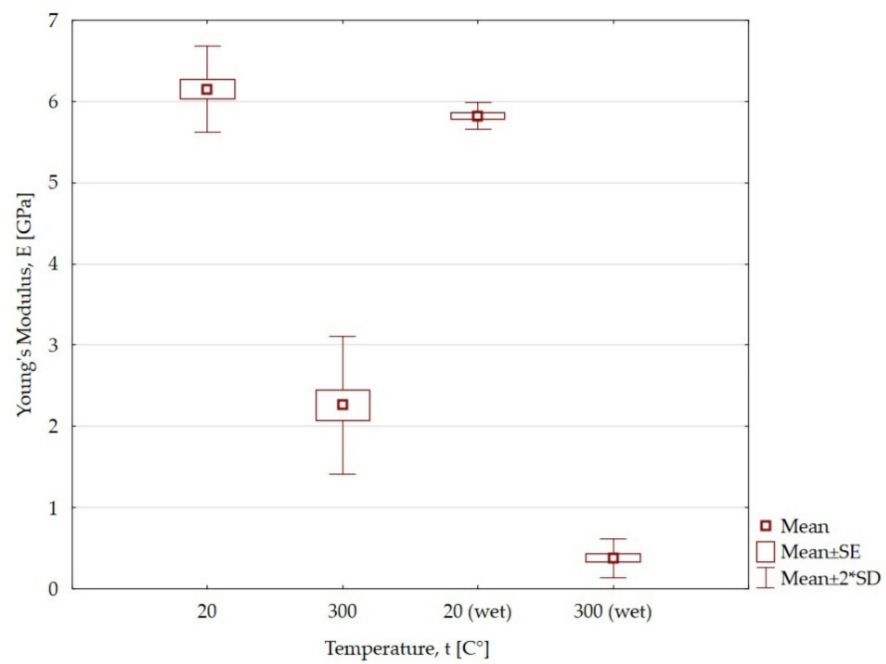


Figure 6. The influence of high temperatures on changes in tensile strength of dry and wet samples: (a) sandstone; (b) claystone; SE—standard error; SD—standard deviation.



(a)



(b)

Figure 7. The influence of high temperatures on the changes in Young's modulus: (a) sandstone; (b) claystone; SE—standard error; SD—standard deviation.

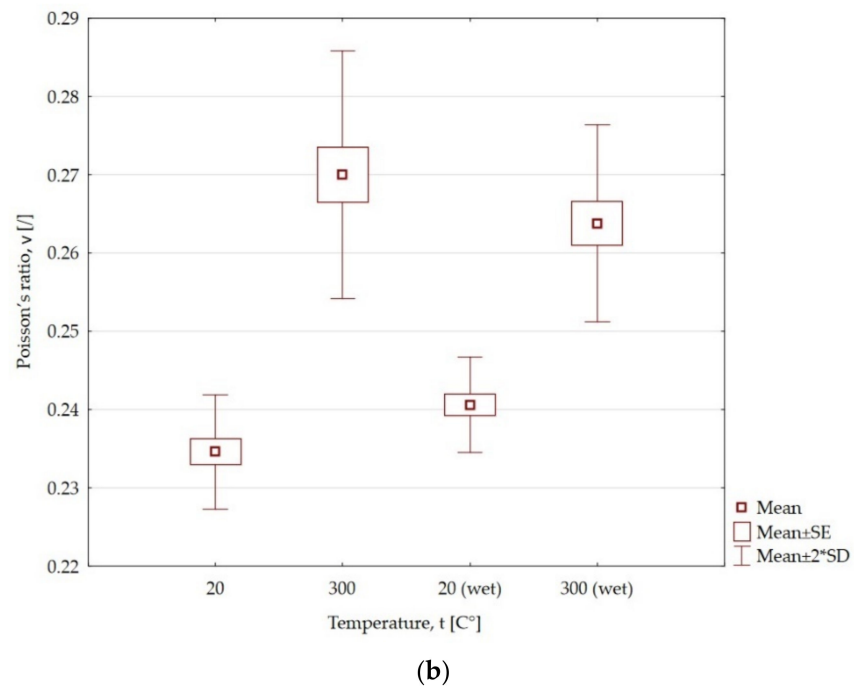
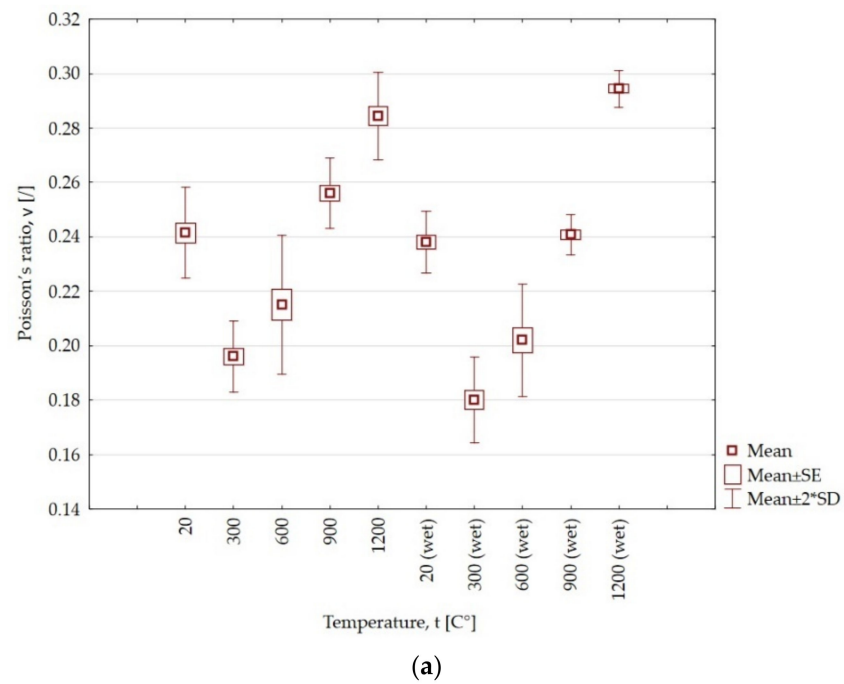


Figure 8. The influence of high temperatures on changes in Poisson's ratio: (a) sandstone; (b) claystone; SE—standard error; SD—standard deviation.

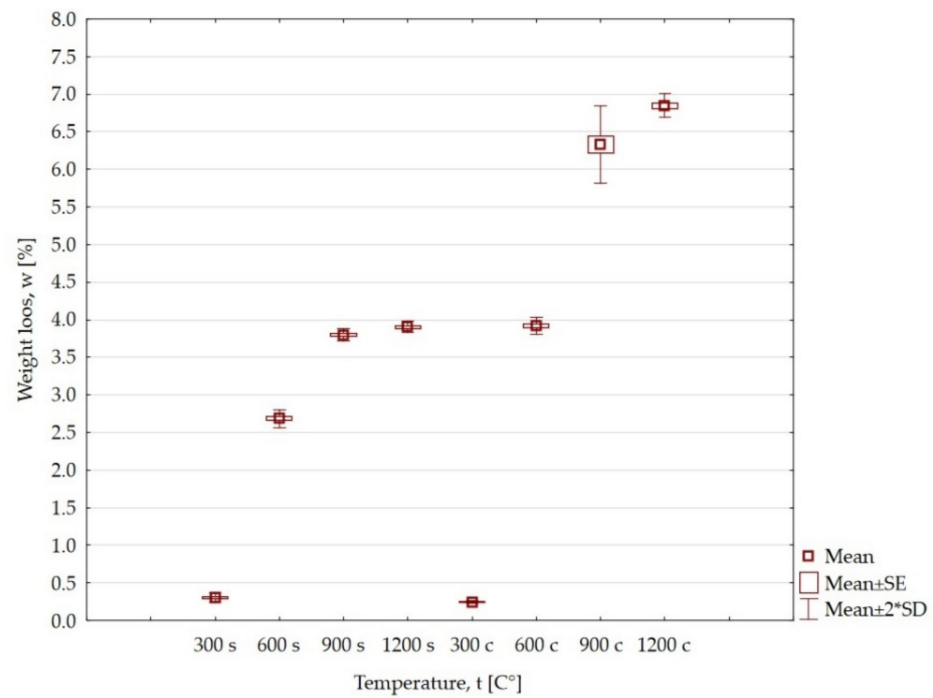


Figure 9. The influence of high temperatures on the weight loss for sandstone and claystone samples: s—sandstone; c—claystone; SE—standard error; SD—standard deviation.

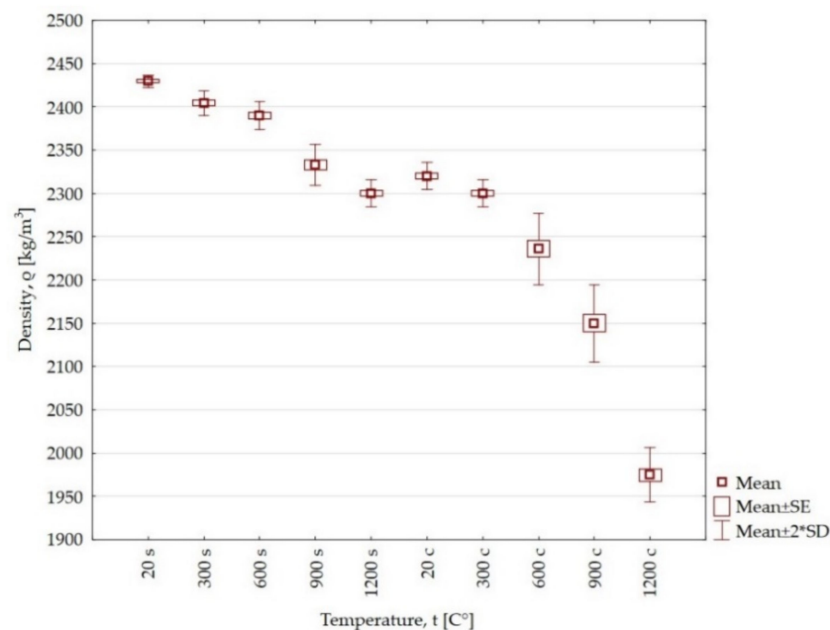


Figure 10. The influence of high temperature on the weight loss for sandstone and claystone samples: s—sandstone; c—claystone; SE—standard error; SD—standard deviation.

The average compressive strength of sandstone samples at 20 °C was 61.2 MPa. Increasing the temperature to 300 °C and 600 °C increased the strength by 80% and 36%, respectively. On the other hand, at the temperatures of 900 °C and 1200 °C, a significant decrease in strength was recorded, by 30% and 65.6%, respectively, in relation to the initial value. For the heated samples, which were then kept in water for 24 h, the range of changes compared to the temperature of 20 °C was an increase of 72% and 7.7% for the temperatures of 300 °C and 600 °C, respectively. The influence of temperature and water caused a drop in strength by 60.7% and 95.7%, respectively, for the temperatures of 900 °C and 1200 °C.

The influence of water on the heated samples caused a decrease in compressive strength by 8%, 28.3%; 30.7% and 30.1%, respectively, for the temperatures of 300 °C, 600 °C, 900 °C and 1200 °C compared to samples that were only heated. In the case of claystone, the influence of the temperature of 300 °C caused a drop in strength by 80.5% and 93.3% for the heated and wet samples, respectively, compared to the initial value. This means that the influence of water contributes to a further decrease in strength by almost 13%.

Tensile strength is one of the basic constants describing the strength properties of rock material, which can be determined using direct and indirect methods in accordance with the recommendations of the International Society for Rock Mechanics and Rock Engineering [29]. Tensile strength tests were carried out using the Brazilian method (transverse compression), in which the tensile force was created in the axial cross-section of a sample, perpendicular to the compressive load. The test specimens had a cylindrical shape with a diameter of 48 mm and a length of 96 mm. The load was transferred from the hydraulic press to the sample by loading platens. Tensile strength could be calculated according to Equation (1) [30]:

$$T_s = \frac{2 \cdot L}{\pi \cdot d \cdot w} = 0.636 \cdot \frac{L}{d \cdot w} \quad (1)$$

where:

T_s —tensile strength (MPa);

L —maximal recorded load (N);

d —the diameter of the specimen (mm),

w —the width of the specimen (mm).

Sandstone at 300 °C and 600 °C increases its tensile strength by 24% and 10.6%, respectively, compared to the initial value. On the other hand, a further increase in temperature to the value of 900 °C and 1200 °C contributes to a decrease in strength by 55.36% and 78.3%, respectively. Even greater differences are found for wet samples. Only for the temperature of 300 °C is there an increase in strength by 19.6%, while for the temperatures of 600 °C, 900 °C and 1200 °C, there is a decrease by 5.37%, 72.8% and 93.45%, respectively. Immersion of the heated sandstone samples in water reduces the tensile strength by 4.4%, 15.97%, 17.44% and 20.15%, respectively, for the temperatures of 300 °C, 600 °C, 900 °C and 1200 °C compared to the only heated samples. The average decrease in tensile strength for claystone heated at 300 °C and treated with water was 55.15% and 75.78% with respect to the temperature of 20 °C. For samples of claystone heated at the temperature of 300 °C, the influence of water is characterized by an over two times decrease in tensile strength.

At the temperature of 300 °C and 600 °C, the value of Young's modulus increases by 3.96 GPa and 1.07 GPa, respectively, compared to the temperature of 20 °C. However, at temperatures of 900 °C and 1200 °C, the value drops and is lower by 5.1 GPa and 8.58 GPa, respectively, compared to the initial value. As a result of the action of water, the Young's modulus decreases by 0.79, 0.75, 1.58 and 1.4 GPa, respectively, for samples only heated at the temperatures of 300 °C, 600 °C, 900 °C and 1200 °C. In the case of claystone heated at 300 °C and when wet, the Young's modulus decreases by 3.89 GPa and 5.44 GPa, respectively. The action of water results in an almost six times lower value of Young's modulus compared to samples only heated for the maximum temperature of claystone.

For sandstone samples heated at 900 °C and 1200 °C, the Poisson's ratio value increases by 6% and 17.8%, respectively, and decreases by 18.8% and 10.9% for the temperatures of 300 °C and 600 °C in relation to the value of 20 °C. On the other hand, for the heated samples exposed to water, the value of the Poisson's ratio for the temperatures of 300 °C and 600 °C decreases by 24.3% and 15.1%, and for the temperatures of 900 °C and 1200 °C, the value increases by 1.1% and 23.6%, respectively. The influence of water on the heated samples reduces the Poisson's ratio by 8.16%, 6.04% and 5.9%, respectively, for the temperatures of 300 °C, 600 °C and 900 °C, and causes an increase of 3.5% for the temperature of 1200 °C. For claystone heated at 300 °C and wet claystone, the value of the Poisson's ratio increases

to 13.1% and to 8.79% in relation to the temperature of 20 °C. As a result of the action of water, the value of the Poisson's ratio drops slightly by 2.29%. The summary of the compressive strength and Poisson's ratio in relation to high temperatures is presented in Table 1.

Table 1. Comparison of the results of compressive strength and Poisson's ratio in relation to high- temperatures.

Type of Rock	Parameter	Temperature, t (°C)				
		20	300	600	900	1200
Sandstone dry	Cs, (MPa)	61.2	110.6	83.6	42.8	21
	ν	0.241	0.196	0.215	0.256	0.284
Sandstone wet	Cs, (MPa)	59.6	103	64.2	23.4	2.54
	ν	0.238	0.18	0.202	0.240	0.294
Claystone dry	Cs, (MPa)	31.8	6.2			
	ν	0.234	0.27			
Claystone wet	Cs, (MPa)	26.8	1.78			
	ν	0.240	0.263			

Cs—compressive strength; ν —Poisson's ratio.

Heating sandstone and claystone at the temperature of 300 °C does not significantly affect the loss of weight. The losses are very small and amount to 0.3% and 0.24%. At the temperatures of 600 °C, 900 °C and 1200 °C, the losses are one order higher compared to the temperature of 300 °C. The loss of mass at these temperatures for claystone in relation to sandstone is greater by 1.24%, 2.53% and 2.94%, respectively.

With increasing temperature, the density of both sandstone and claystone decreases. However, much greater changes occur for claystone samples. For both rocks heated at the temperature of 300 °C, the change in density is at a similar level and amounts to about 1%. On the other hand, at the temperatures of 600 °C, 900 °C and 1200 °C, there is a further reduction in density, with the changes being greater for claystone by 1.98%, 3.35% and 9.54% compared to the sandstone samples.

4. Numerical Modeling

The main goal of numerical modeling was to determine the extent of the rock destruction zone around the gasification channel. For this purpose, RS2 [31] software was used, which is based on the finite element method. For the evaluation of the damage zones, the strength factor was selected, expressing the ratio of the rock strength to the reduced stresses at a given point. Strength factor values below 1 indicate material failure. The modeling adopted the Hoek–Brown criterion, which links the compressive strength and material constants determined using RocData software [31]. The results obtained from the laboratory tests were used in numerical simulations. A square target with a side length of 100 m was adopted in the modeling. In numerical modeling, it was assumed that the horizontal and vertical stresses are equal to each other: $\sigma_1 = \sigma_3 = \sigma_z = 23.3$ MPa. The adoption of such a value resulted from the depth of the hard coal deposit and the unit weight of the overburdened rocks. The size of the model was selected so that for the largest width of the gasification channel, equal to 30 m, the extent of rock destruction could be recorded. The models adopted a graded mesh and six-noded triangles with a gradation factor equal to 0.1. The number of nodes on all excavations was equal to 110. The models were restrained on all sides. As most of the claystone samples were destroyed under the influence of the temperature of 300 °C (Figure 3), the modeling assumed that the height of the gasification channel was 1.5 m. This height consisted of the thickness of the coal seam equal to 0.4 m and the total destruction of claystone rocks in the roof and the floor with a total thickness of 1.1 m (Figure 1). In the numerical simulations, three widths of

the gasification channel, 10, 20 and 30 m (Figure 11a–c), were adopted. In addition, three ranges, 0.5, 1.0 and 1.5 m (Figure 11d–f), for the effects of high temperatures both in the roof and floor of the coal seam were modeled. The test results are shown in Figures 12–17 and Table 2.

Table 2. Summary of the results of the range of the rock destruction zone around the gasification channel.

Channel Width, (m)	Temperature Impact Range (m)				The Maximum Extent of the Rock Destruction Zone around the Gasification Channel for a Dry Rock Mass (m)		The Maximum Extent of the Rock Destruction Zone around the Gasification Channel for a Wet Rock Mass (m)	
	1200 °C	900 °C	600 °C	300 °C	Roof	Floor	Roof	Floor
	10	0.5	1.0	1.5	2.0	4.51	4.36	5.0
1.0		2.0	3.0	4.0	4.58	4.47	5.18	5.08
1.5		3.0	4.5	6.0	4.63	4.54	5.52	5.32
20	0.5	1.0	1.5	2.0	8.96	8.60	9.75	9.23
	1.0	2.0	3.0	4.0	9.33	8.87	10.58	9.96
	1.5	3.0	4.5	6.0	9.49	9.04	10.92	10.30
30	0.5	1.0	1.5	2.0	14.06	12.91	15.27	13.98
	1.0	2.0	3.0	4.0	14.29	13.43	16.09	15.08
	1.5	3.0	4.5	6.0	14.72	13.70	16.83	15.58

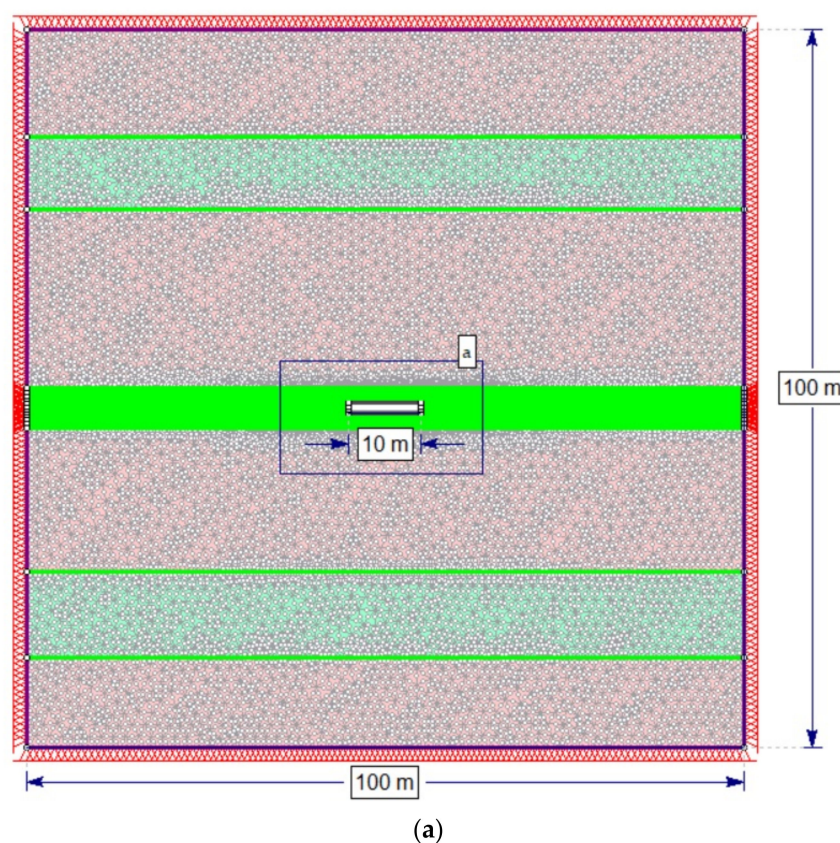
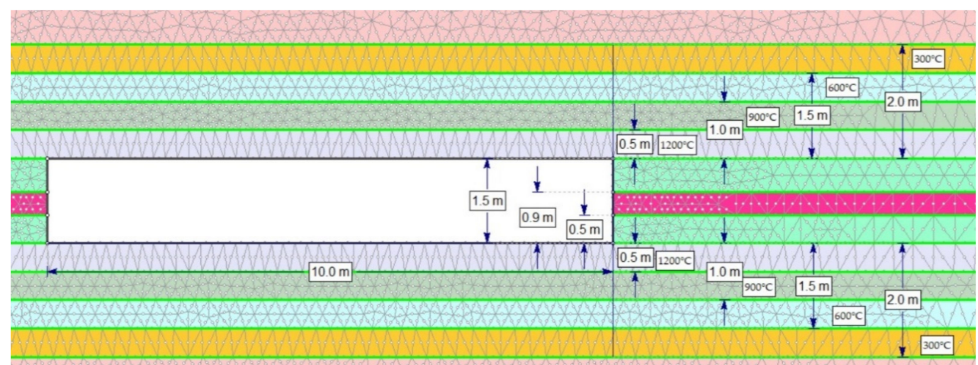
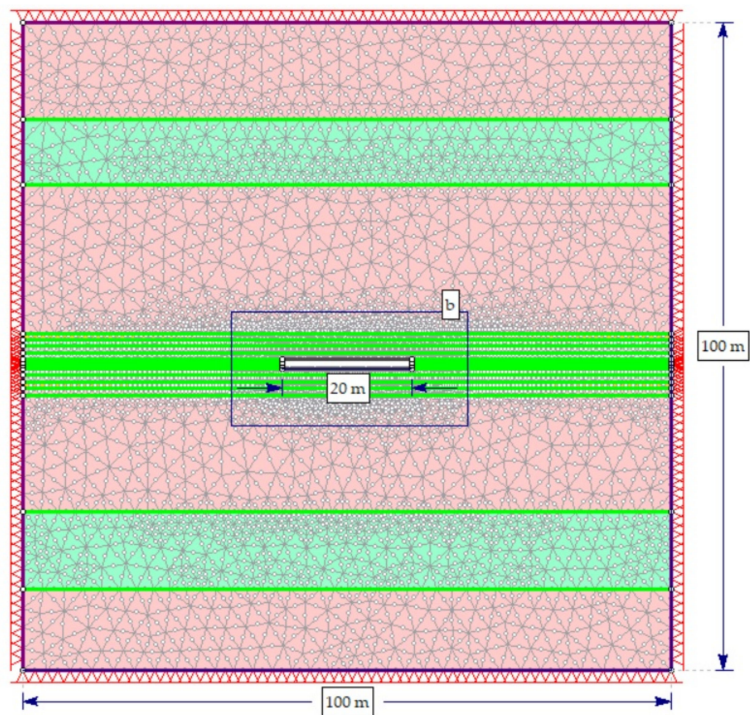


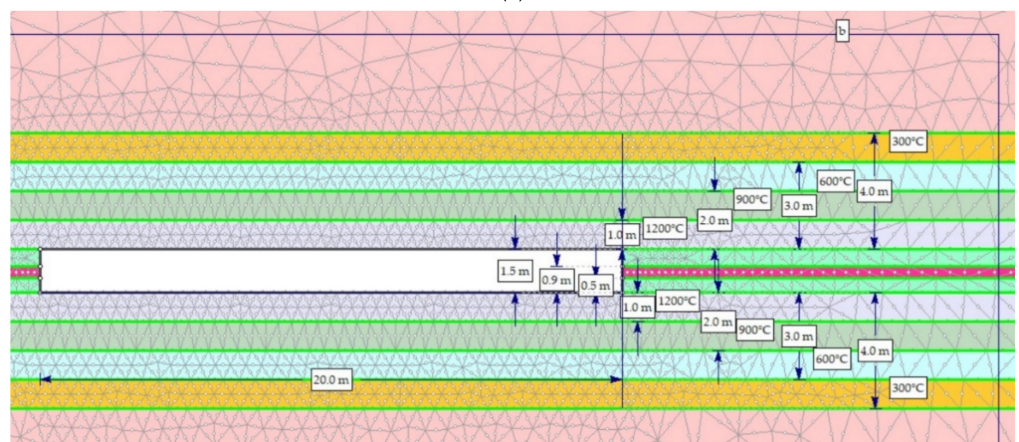
Figure 11. Cont.



(b)



(c)



(d)

Figure 11. Cont.

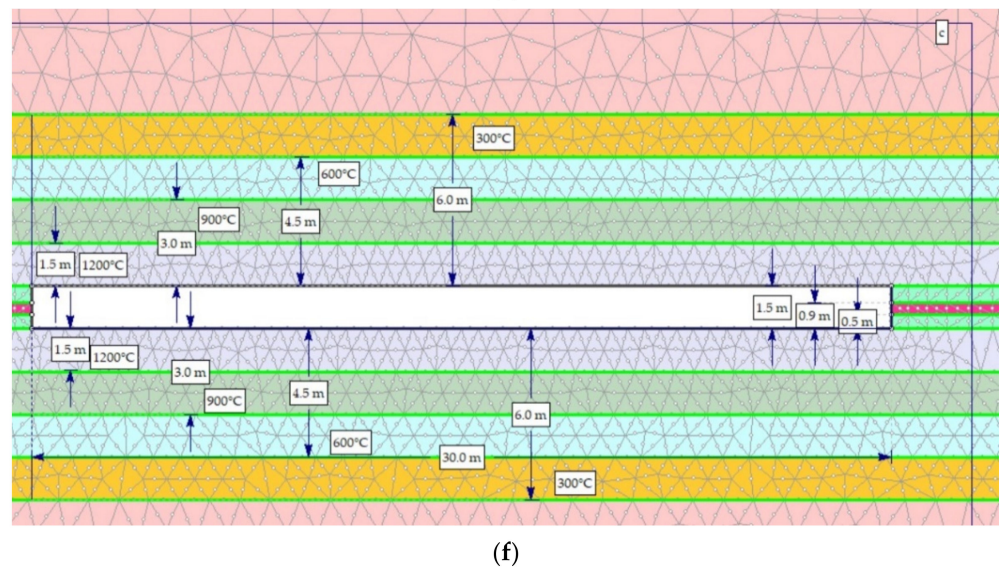
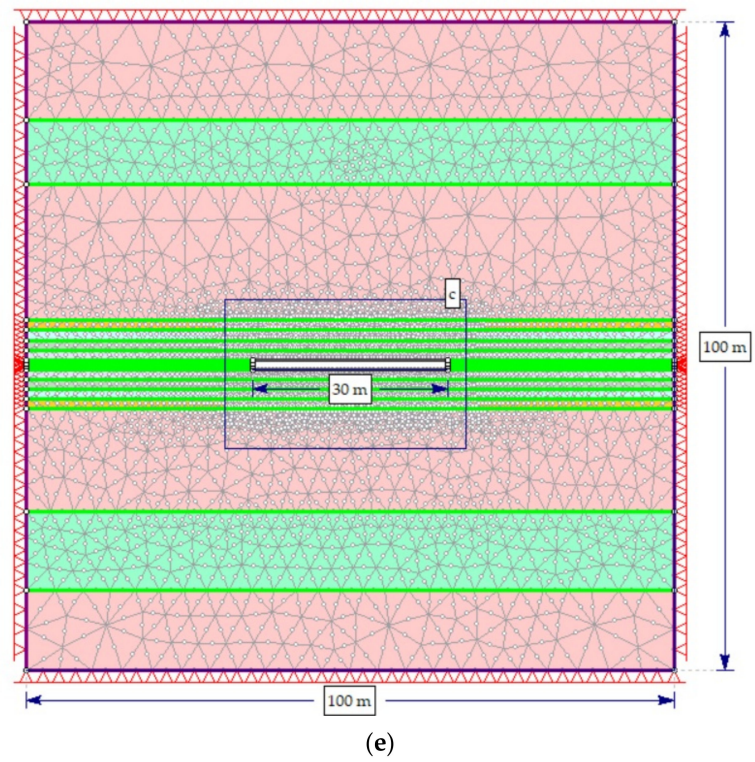
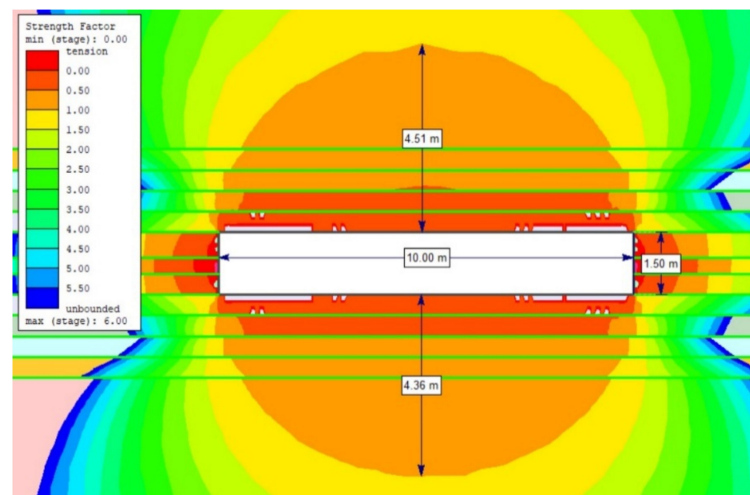
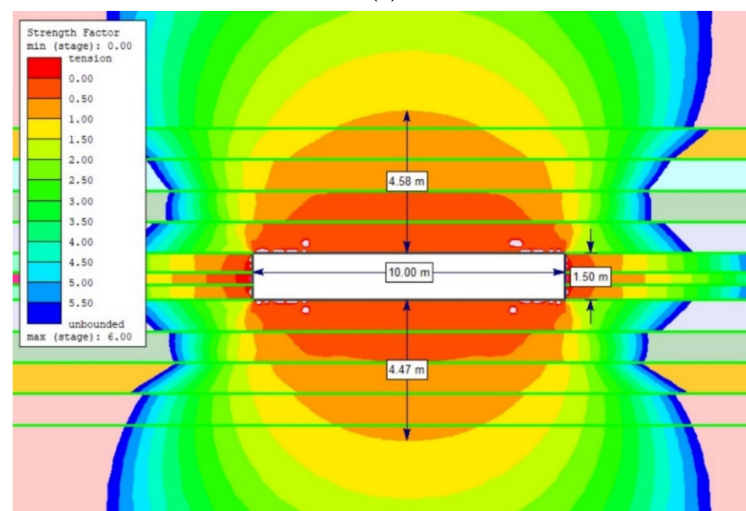


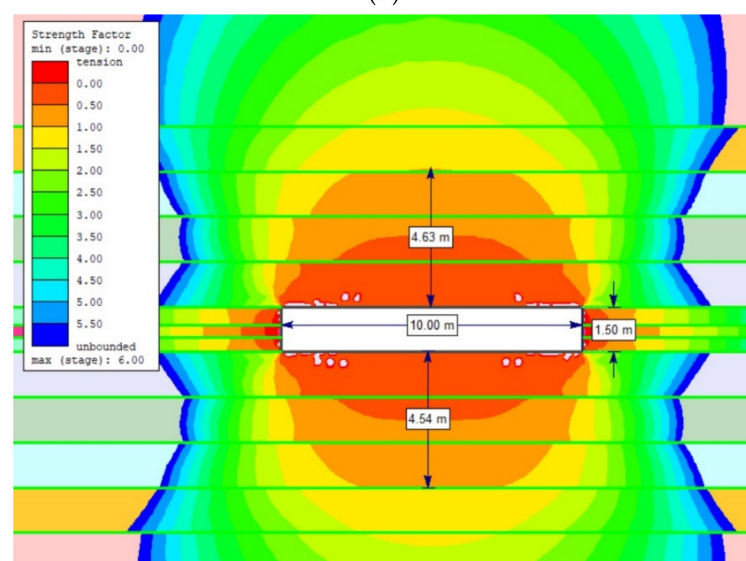
Figure 11. Numerical models: (a) channel width 10 m; (b) detail “a”; (c) channel width 20 m; (d); detail “b”; (e) channel width 30 m; (f) detail “c”.



(a)

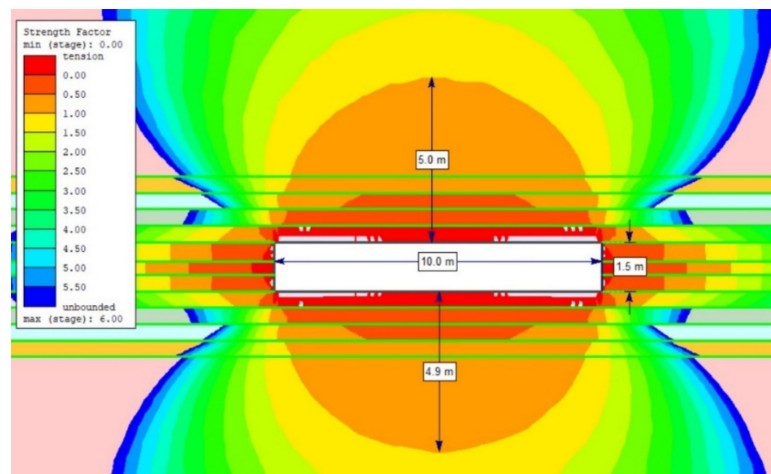


(b)

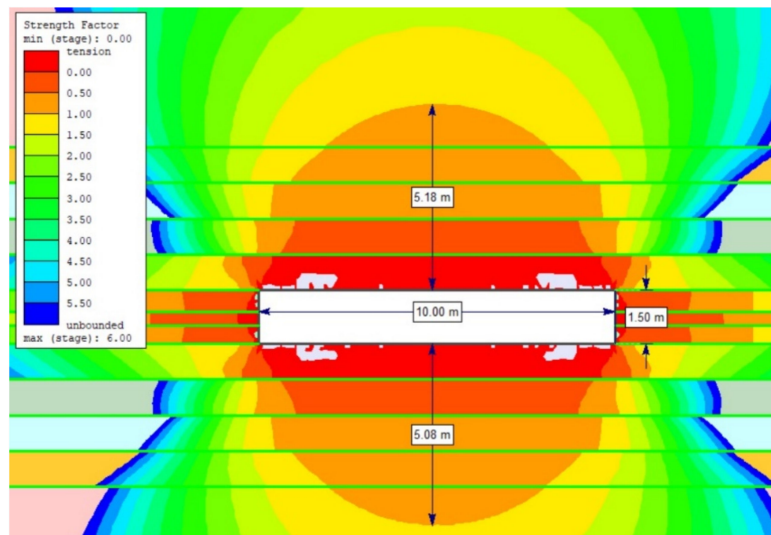


(c)

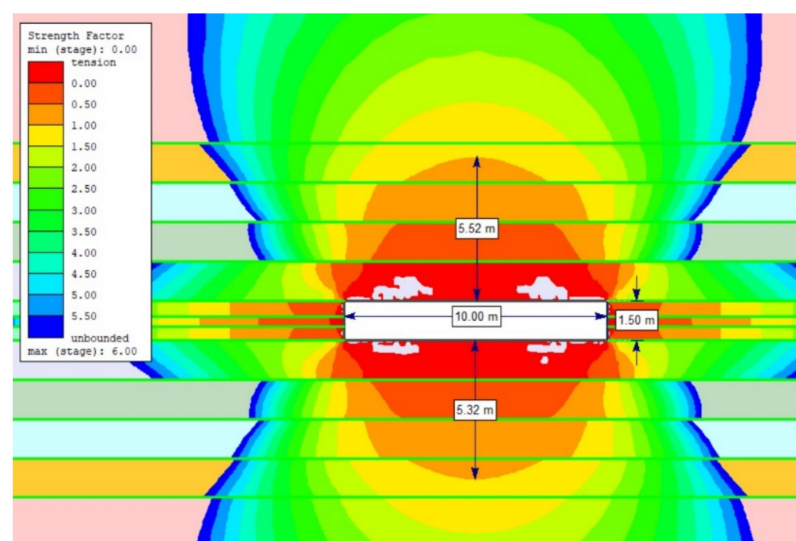
Figure 12. The extent of the rock destruction zone around the gasification channel with a width of 10 m and the impact of temperature of 1200 °C for the dry rock mass, up to the height of: (a) 0.5 m; (b) 1.0 m; (c) 1.5 m.



(a)

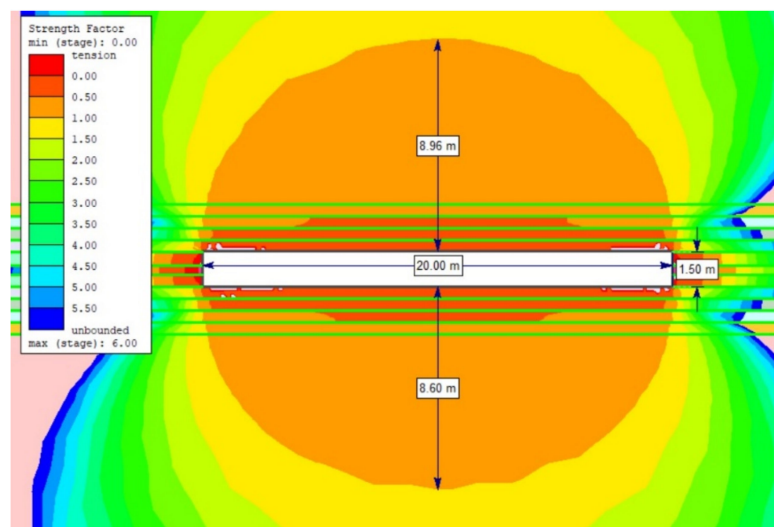


(b)

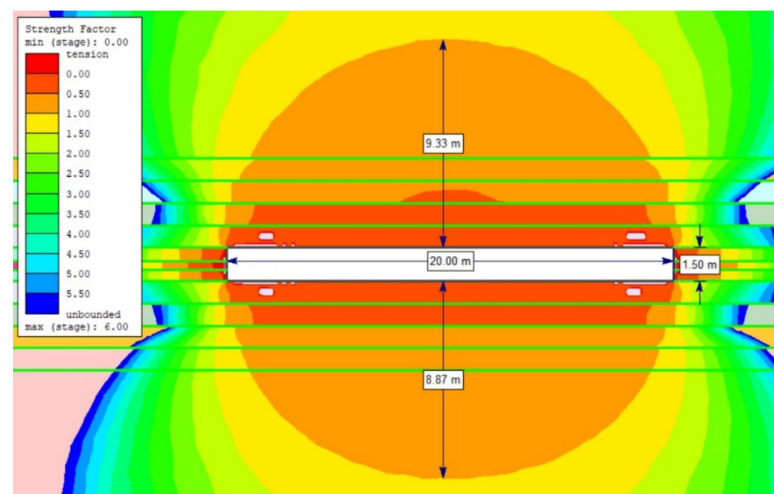


(c)

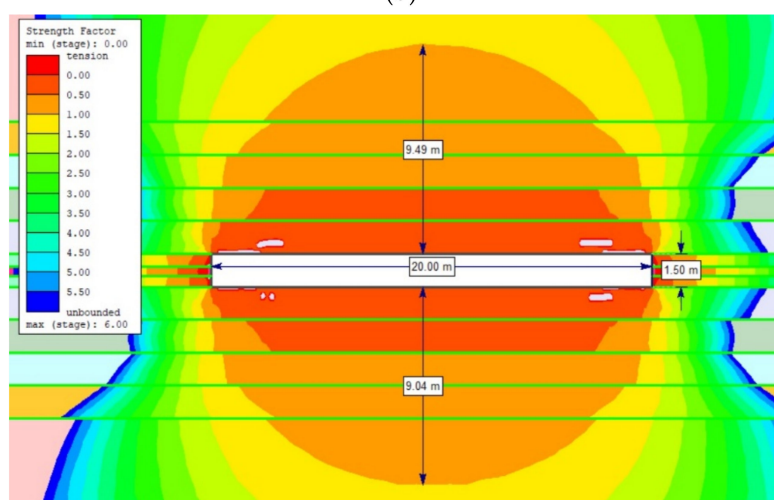
Figure 13. The extent of the rock destruction zone around the gasification channel with a width of 10 m and the impact of temperature of 1200 °C for the wet rock mass, up to the height of: (a) 0.5 m; (b) 1.0 m; (c) 1.5 m.



(a)

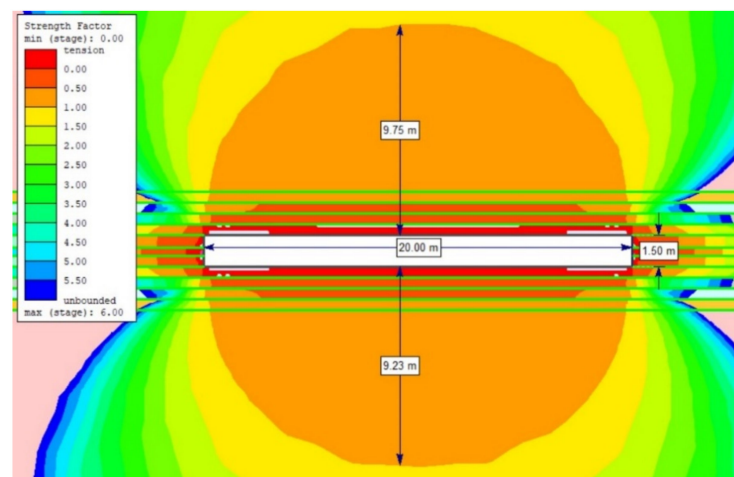


(b)

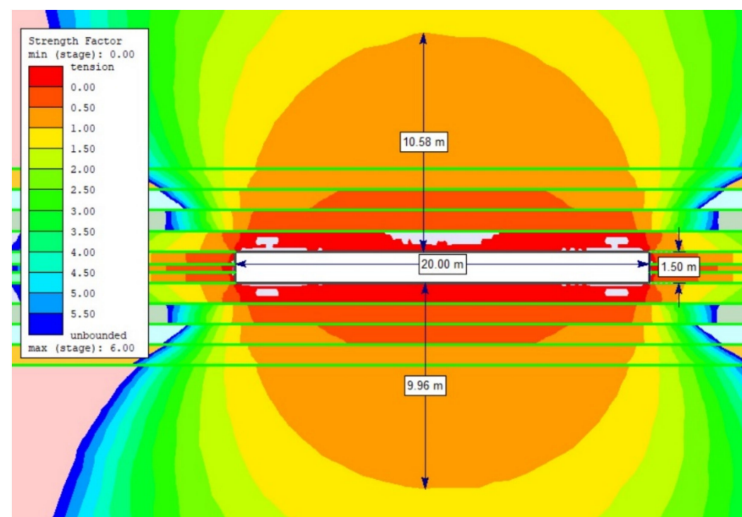


(c)

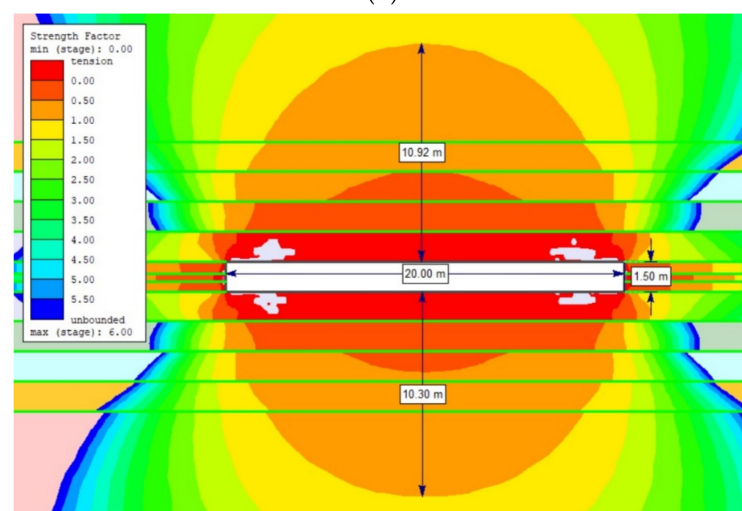
Figure 14. The extent of the rock destruction zone around the gasification channel with a width of 20 m and the impact of temperature of 1200 °C for the dry rock mass, up to the height of: (a) 0.5 m; (b) 1.0 m; (c) 1.5 m.



(a)

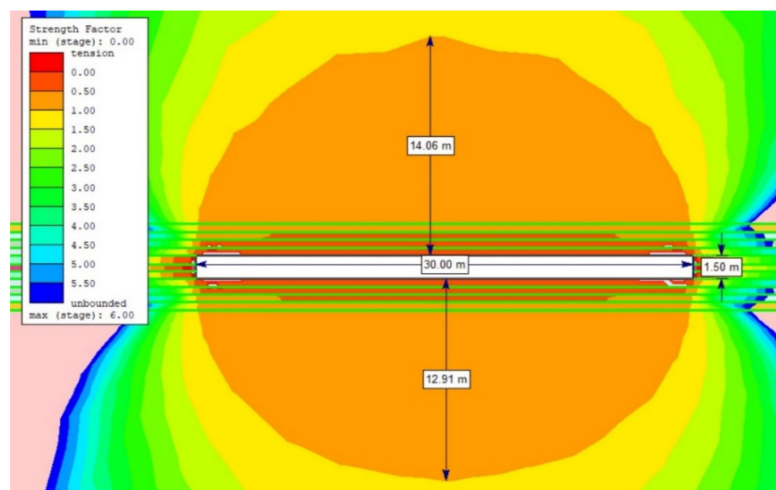


(b)

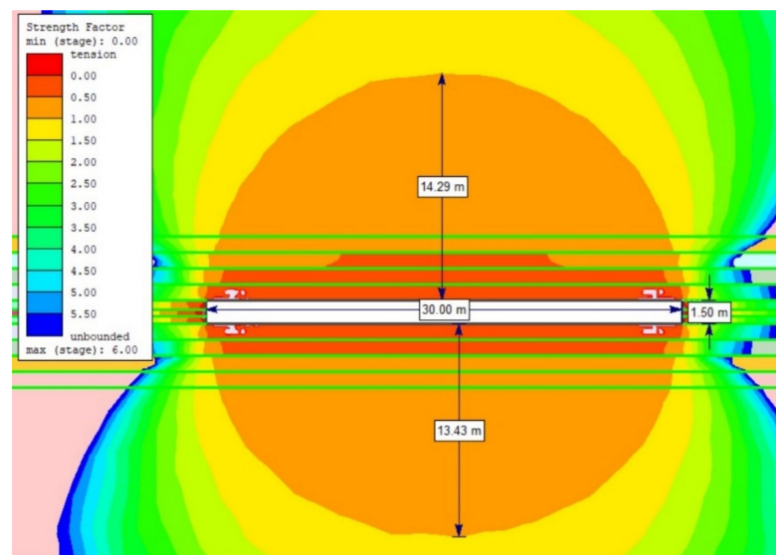


(c)

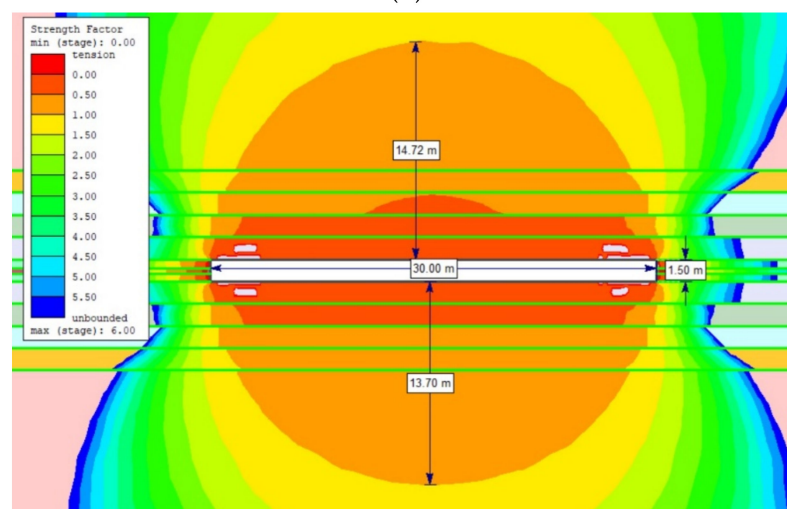
Figure 15. The extent of the rock destruction zone around the gasification channel with a width of 20 m and the impact of temperature of 1200 °C for the wet rock mass, up to the height of: (a) 0.5 m; (b) 1.0 m; (c) 1.5 m.



(a)

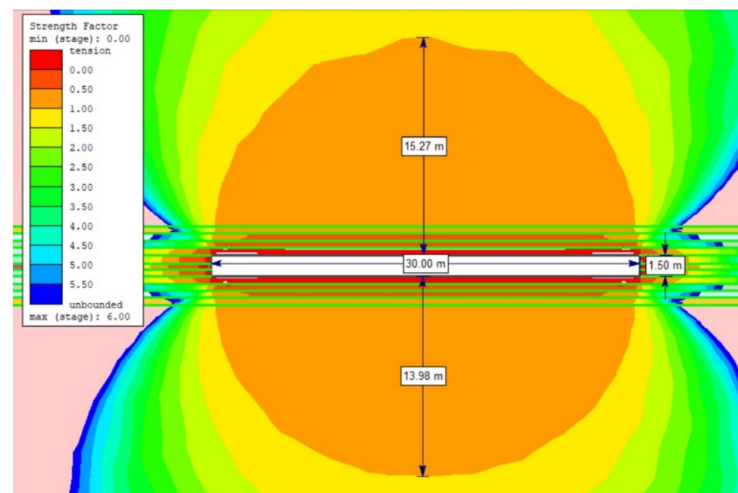


(b)

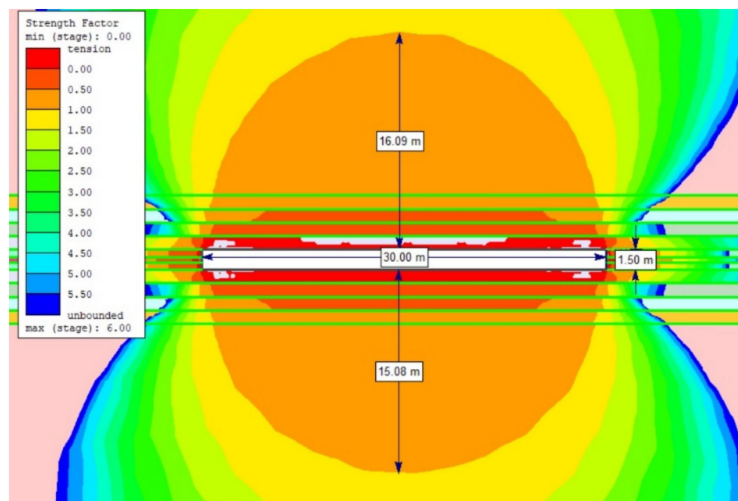


(c)

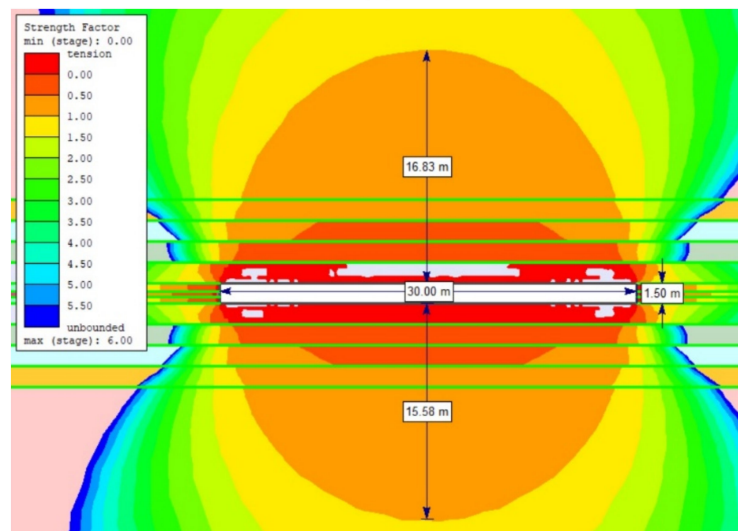
Figure 16. The extent of the rock destruction zone around the gasification channel with a width of 30 m and the impact of temperature of 1200 °C for the dry rock mass, up to the height of: (a) 0.5 m; (b) 1.0 m; (c) 1.5 m.



(a)



(b)



(c)

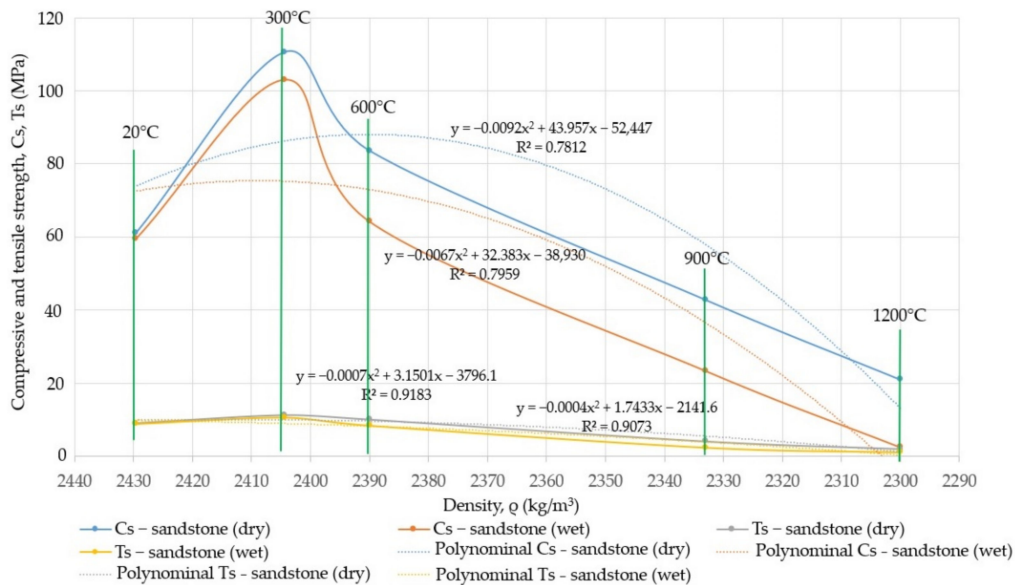
Figure 17. The extent of the rock destruction zone around the gasification channel with a width of 30 m and the impact of temperature of 1200 °C for the wet rock mass, up to the height of: (a) 0.5 m; (b) 1.0 m; (c) 1.5 m.

5. Discussion

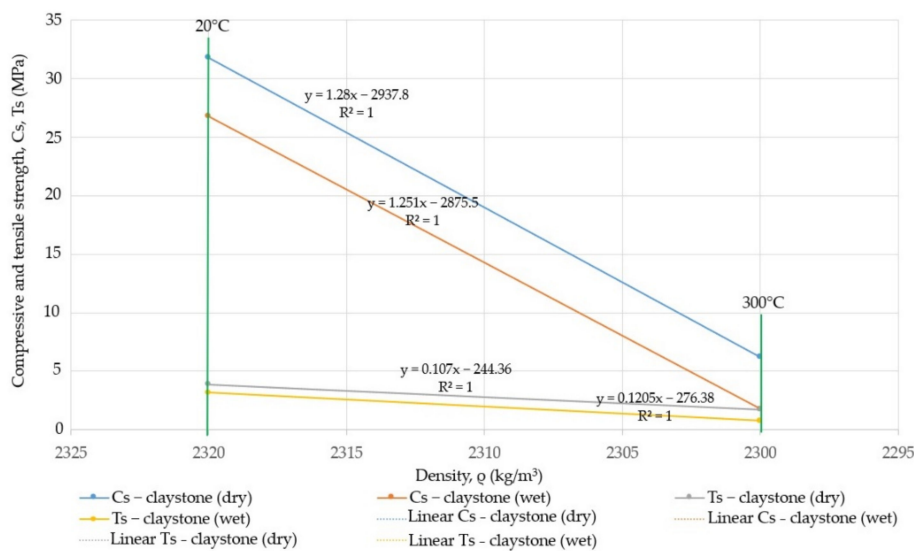
The process of underground coal gasification takes place in underground generators, which can be prepared using shaft and non-shaft methods. In the shaft method, mining excavations are performed underground after the coal seam is made available through a vertical and inclined shaft. In the structure of accessibility, the workings of the mine are used to supply an oxidizing agent and discharge gas to the surface. The oxidizing agent may be supplied to the coal seam by means of: roadway inside the body of coal; through holes made in the body of coal between roadways; and blind holes to which the oxidizing agent is led through heat-resistant pipes [32]. The main advantage of this method is the accuracy of recognizing the conditions of the coal seam, easy drainage of the deposit and verification of the influence of high temperatures on the surrounding rock layers. On the other hand, the disadvantage is the cost of construction and the maintenance of access and preparatory workings. In the non-shaft method, the coal seam is made available through vertical, inclined and directional holes from the surface, and then they are joined together [33]. Vertical holes are used in the execution of the initial front line of fire and drainage of generators. Inclined holes are used when it is necessary to arrange them outside the zone of rocks with low strength parameters. Directional holes are a combination of access and generator holes, which are made in horizontal locations or at a slight angle.

Macroscopic observations of carboniferous rock samples taken from a closed hard coal mine in the Upper Silesian Coal Basin, heated at temperatures up to 1200 °C and exposed to water, show that sandstones are not subject to decomposition. Tian et al. [34] noticed that sandstone heated at 1000 °C does not lose its cohesion. Claystone samples, when heated to a temperature of 300 °C, burn out and break into small pieces. Wolf et al. [35] found that for claystone samples, the weight loss is due to, inter alia, the dehydroxylation of clays. Hetema et al. [36] determined that for claystone samples, the compaction number increased with increasing temperature. The influence of water on the heated sandstone samples at a temperature of 1200 °C contributes to the reduction in strength, deformation and structural parameters by 87% (compressive strength), 70% (tensile strength), 73% (Young's modulus) and 5.3% (density). The value of the Poisson's ratio is at a similar level; at 1200 °C, it slightly increases by 3.5%. Wu et al. [37] also confirmed the increase in Poisson's ratio after exceeding the temperature of 1000 °C. The behavior of rocks under the influence of heat and water is very diverse. Bresser et al. [38] discovered that for marbles heated at 600 °C, the influence of water on the change of strength parameters is small. Luo et al. [39] noted that the value of modulus of elasticity and compressive strength for mudstone at 200 °C ÷ 600 °C is at a similar level, followed by their increase. Kiliç [40] pointed out that for limestone samples, the weight loss process starts at 600 °C, whereas for sandstone and claystone samples, the weight loss is 2.6% and 3.9%, respectively. Zhang et al. [41] found that sandstone increases its compressive strength to a temperature of 500 ÷ 600 °C, followed by a drop in strength by several dozen percent. In turn, Rao et al. [42] noticed that sandstone increases its tensile strength to a temperature of 250 °C. The increase in compressive strength of sandstone samples is related to the mineralogical composition. The main component of sandstone is quartz, for which the melting point is above 1410 °C. At temperatures up to 300 °C, the dehydroxylation of iron oxides and hydroxides or organic matter oxidation can occur. On the other hand, up to the temperature of 600 °C, water vapor is released in the amount of several grams per kilogram of sample. The main mineralogical changes in sandstones as a result of high temperatures are the appearance of hematite and ore minerals and a reduction in the amount of heavy minerals [43]. The tensile strength, determined by the Brazilian method, is significantly influenced by the cross-sectional area along which the fracture occurs. This influence is conditioned by both surface and volumetric factors, with the volumetric effect being of decisive importance. It depends on the mineral composition, structure and texture of the rock and, above all, the sum of structural defects, in particular fracture and cleavage. Thus, the volume factor expresses the sum of the structural defects of the rock within a given volume, while the surface factor determines the condition of the potential fracture surface. For claystone rocks, both of the

described factors appeared at the temperature of 300 °C, which resulted in a significant reduction in tensile strength. For sandstone rocks, the influence of the volumetric and surface factors was revealed only at the temperature of 900 °C. Undoubtedly, the change of strength parameters is significantly influenced by carbon substance lamines, which, when exposed to high temperature, burn out and directly reduce the tensile strength, especially in claystone rocks. The dependence of the compressive strength and tensile strength in relation to the decrease in density is shown in Figure 18a,b.



(a)



(b)

Figure 18. The dependence of the compressive strength and tensile strength in relation to the decrease in density for: (a) sandstone; (b) claystone.

For sandstone rocks heated at temperatures from 300 °C to 600 °C, the strength parameters increased by 80.7% and 36.6%, respectively (compressive strength for dry rocks); by 72.8% and 7.7%, respectively (compressive strength for wet rocks), by 24.06% and 10.06%, respectively (tensile strength for dry rocks); an increase of 19.63% and a decrease of 5.37% (tensile strength for wet rocks), accompanied by a decrease in density by 1.03% and 1.62%, respectively. For the temperatures of 900 °C to 1200 °C, the compressive strength

decreased by 30.06% and 65.68% (for dry rocks) and 60.73% and 95.73% (for wet rocks), respectively. In the case of tensile strength, also for these temperatures, there was a decrease by 55.36% and 78.32 (for dry rocks) and 72.86% and 87.29% (for wet rocks), respectively, which was accompanied by a decrease in density by 3.97% and 5.33%, respectively. For claystone rocks heated to the temperature of 300 °C, both in the case of compressive strength and tensile strength, the value decreased by 80.5% (compressive strength dry) and 93.35% (compressive strength wet) and 55.15% (tensile strength dry) and 75.78% (tensile strength wet), accompanied by a decrease in density by 0.86%. A further increase in temperature to the values of 600 °C, 900 °C and 1200 °C contributed to a decrease in density by 3.62%, 7.32% and 14.87%, respectively, with the simultaneous destruction of the integrity of the samples, making it impossible to determine the strength parameters.

In the model studies conducted by Otto et al. [44] and Nakaten et al. [45], the width of the gasification channel was often assumed to be 20 m. Pivnyak et al. [46] determined that the range of the impact of high temperature in the roof and floor can reach values up to 5.7 and 3.2 thickness of the gasified coal seam, respectively. Experiments conducted in Russia showed that, depending on the type of rock, due to the heating of the roof, rocks in the cave zone may be in the range of 1.33–3.8 m, and the metamorphized zone of rocks is from 0.65 m to 0.84 m [47]. Luo et al. [48], based on numerical simulations, determined that the temperature of 900 °C can have a range of up to 9 m in the roof. On the other hand, Wiatowski et al. 2021 [49], based on research on large samples of hard coal, found that when there is a siderite layer in the coal seam, the maximum temperature of 1200 °C occurs at a distance of 0.3 m above the gasified seam. As a result of the high temperature, the roof rocks, in particular claystone, can fall downwards, making it possible for gases to migrate into the rock mass and cause an increase in the temperature of the surrounding rocks. Moreover, as a result of high temperature, the geometry of the carbon pillars changes, which translates into an increase and change in the stress distribution around the gasification channel [50].

6. Conclusions

Based on the laboratory tests of rock samples heated at high temperatures, it can be concluded that:

- For dry claystone at the temperature of 300 °C, the compressive strength and tensile strength decrease by 80.5% and 55.15%, respectively, while for wet claystone, these decrease by 93.35% and 75.78%, respectively, in relation to the initial value. After exceeding the temperature of 300 °C, the claystone decomposed;
- For dry sandstone heated at 300 °C and 600 °C, the compressive strength increases by 80.7% and 36.6%, respectively, while for temperatures from 900 °C to 1200 °C, there is a decrease by 30.06% and 65.68%, respectively, in relation to the temperature of 20 °C. In the case of wet sandstone, there is an increase of 72.8% and 7.7% for temperatures of 300 °C and 600 °C, respectively, and a decrease of 60.73% and 95.73%, respectively, for temperatures of 900 °C and 1200 °C. The tensile strength for dry sandstone increases by 24.06% and 10.06%, respectively, for the temperatures of 300 °C and 600 °C, and decreases by 30.06% and 65.68%, respectively, for the temperatures of 900 °C and 1200 °C. On the other hand, for wet sandstone, there is an increase of 19.63% for the temperature of 300 °C and a decrease of 5.37%, 72.86% and 87.29% for the temperatures of 600 °C, 900 °C and 1200 °C, respectively;
- Within the temperature range of 300 °C, 600 °C, 900 °C, 1200 °C, the density decreases by 0.86%, 3.62%, 7.32% and 14.87%, respectively, for claystone rocks, and 1.03%, 1.62%, 3.97% and 5.33%, respectively, for sandstone compared to the initial value.
- Based on numerical research, it can be concluded that:
- For the width of the gasification channel equal to 10, 20 and 30 m, the maximum extent of rock destruction for dry rock mass does not exceed 5, 10 and 15 m, respectively;
- An increase in the extent of rock destruction occurs for wet rock mass. For roof rocks, the maximum range is increased by 19.2%, 15% and 14.33%;

- Additionally, for floor rocks, there is an increase by 17.1%, 13.9% and 13.7% in relation to the dry rock mass.

Rocks located in the immediate vicinity of the designed georeactor are the basis for its stability analyses. The conducted research shows a strong dependence of certain values of the strength parameters of carboniferous rocks on high temperature, which in the process of underground coal gasification often exceeds 900 °C. The obtained results regarding the extent of the rock destruction zone around the gasification channel indicate the need to conduct this process in a strongly controlled manner, because the extent of rock destruction increases with the increase in the width of the gasification channel. The existence of underground water reservoirs and the possibility for water to tear through the fractured rock mass additionally reduces the strength parameters of the heated rocks and increases the extent of rock destruction.

Author Contributions: Conceptualization, K.S. and K.Z.; methodology, K.S. and K.Z.; software, K.S.; validation, K.S., K.Z. and A.Z.; formal analysis, K.S., K.Z. and A.Z.; investigation, K.S., K.Z. and A.Z.; resources, K.S.; data curation, K.S., K.Z. and A.Z.; writing—original draft preparation, K.S. and K.Z.; writing—review and editing, K.S., K.Z. and A.Z.; visualization, K.S., K.Z. and A.Z.; supervision, K.S., K.Z.; project administration, K.S., K.Z.; funding acquisition, K.S., K.Z. All authors have read and agreed to the published version of the manuscript.

Funding: This research was prepared as part of AGH University of Science and Technology in Poland, scientific subsidy under number: 16.16.100.215.

Institutional Review Board Statement: Not applicable.

Informed Consent Statement: Not applicable.

Data Availability Statement: The data presented in this study are new and have not been previously published.

Conflicts of Interest: The authors declare no conflict of interest.

References

1. Kostúr, K.; Laciak, M.; Durdan, M. Some Influences of Underground Coal Gasification on the Environment. *Sustainability* **2018**, *10*, 1512. [CrossRef]
2. Dubiński, J.; Turek, M. Basic aspects of productivity of underground coal gasification proces. *Archi. Min. Sci.* **2015**, *2*, 443–453.
3. Sajjad, M.; Rasul, M.G. Prospect of Underground Coal Gasification in Bangladesh. *Procedia Eng.* **2015**, *105*, 537–548. [CrossRef]
4. Ordinance of the Minister of the Environment of June 20, 2005 Changing the Ordinance on the Criteria for the Balance of Mineral Deposits. Available online: <https://www.prawo.pl/akty/dz-u-2005-116-978,17199479> (accessed on 26 August 2021).
5. Kapusta, K.; Stańczyk, K. Pollution of water during underground coal gasification of hard coal and lignite. *Fuel* **2011**, *90*, 1927–1934. [CrossRef]
6. Kapusta, K.; Stańczyk, K.; Korczak, K.; Pankiewicz, M.; Wiatowski, M. Some aspects of impact of underground coal gasification process on water environment. *Res. Rep. Min. Environ.* **2010**, *4*, 17–27. (In Polish)
7. Liu, S.; Wang, Y.; Yu, L.; Oakey, J. Volatilization of mercury, arsenic and selenium during underground coal gasification. *Fuel* **2006**, *85*, 1550–1558. [CrossRef]
8. Chmura, K. *Physico-Thermal Properties of Rocks of Some Polish Mining Basins*; Śląsk Publishing House: Katowice, Poland, 1970; p. 63. (In Polish)
9. Tian, H.; Mei, G.; Jiang, G.S.; Qin, Y. High-Temperature Influence on Mechanical Properties of Diorite. *Rock Mech. Rock Eng.* **2017**, *50*, 1661–1666. [CrossRef]
10. Liu, X.; Guo, G.; Li, H. Study on the propagation law of temperature field in surrounding rock of underground coal gasification (UCG) combustion cavity based on dynamic thermal parameters. *Results Phys.* **2019**, *12*, 1956–1963. [CrossRef]
11. Perkins, G. Underground coal gasification Part II: Fundamental phenomena and modeling. *Prog. Energy Combust. Sci.* **2018**, *67*, 234–274. [CrossRef]
12. Min, X.; Lin, X.; Weitao, L.; Xiangming, H.; Weimin, C.; Chao, L.; Zhigang, W. Study on the physical properties of coal pyrolysis in underground coal gasification channel. *Powder Technol.* **2020**, *376*, 573–592.
13. Feng, B.; Bhatia, S.K. Variation of the pore structure of coal chars during gasification. *Carbon* **2003**, *41*, 507–523. [CrossRef]
14. Deming, Z.; Wenwen, W.; Libo, L.; Hui, J.; Liejin, G. Variation of pore structure in Zhundong coal particle with stepped K₂CO₃ loading during supercritical water gasification. *Fuel* **2021**, *305*, 1–8.
15. Brotóns, V.; Tomás, R.; Ivorra, S.; Alarcón, J.C. Temperature influence on the physical and mechanical properties of a porous rock: San Julian's calcarenite. *Eng. Geol.* **2013**, *167*, 117–127. [CrossRef]

16. Yavuz, H.; Demirgas, S.; Caran, S. Thermal effect on the physical properties of carbonate rocks. *Int. J. Rock Mech. Min. Sci.* **2010**, *47*, 94–103. [CrossRef]
17. Chaki, S.; Takarli, M.; Agbodjan, W.P. Influence of thermal damage on physical properties on a granite rock: Porosity, permeability and ultrasonic wave evolutions. *Constr. Build Mater.* **2008**, *22*, 1456–1461. [CrossRef]
18. Tian, H.; Kempka, T.; Xu, N.X.; Ziegler, M. Physical properties of sandstone after high temperature treatment. *Rock Mech. Rock Eng.* **2012**, *45*, 1113–1117. [CrossRef]
19. Małkowski, P.; Niedbalski, Z.; Hydzik-Wiśniewska, J. The change and structural thermal properties of rocks exposed to high temperature in the vicinity of designed geo-reactor. *Archi. Min. Sci.* **2013**, *58*, 465–480.
20. Yang, L.; Liang, J.; Yu, L. Clean Coal technology—Study on the pilot Project experiments of underground coal gasifications. *Energy* **2003**, *28*, 1445–1460. [CrossRef]
21. Kacur, J.; Laciak, M.; Durdán, M.; Flegner, P. Model-Free Control of UCG Based on Continual Optimization of Operating Variables: An Experimental Study. *Energies* **2021**, *14*, 4323. [CrossRef]
22. Sygała, A.; Bukowska, M. Identification of temperature effect on post-critical geomechanical properties of loaded sandstones. *Arab. J. Geosci.* **2019**, *12*, 1–10. [CrossRef]
23. Otto, C.; Kempka, T. Thermo-Mechanical Simulations of Rock Behavior in Underground Coal Gasification Show Negligible Impact of Temperature-Dependent Parameters on Permeability Changes. *Energies* **2015**, *8*, 5800–5827. [CrossRef]
24. Hsu, C.; Davies, P.T.; Wagner, N.J.; Kauchali, S. Investigation of cavity formation in lump coal in the context of underground coal gasification. *J. South. Afr. Inst. Min. Metall.* **2014**, *114*, 305–309.
25. Zagorščaka, R.; Sadasivama, S.; Thomas, H.R.; Stańczyk, K.; Kapusta, K. Experimental study of underground coal gasification (UCG) of a high-rank coal using atmospheric and high-pressure conditions in an ex-situ reactor. *Fuel* **2020**, *270*, 117490. [CrossRef]
26. Yang, L.; Zhang, X.; Lis, S.; Yu, L.; Zhang, W. Field test of large-scale hydrogen manufacturing from underground coal gasification (UCG). *Int. J. Hydrog.* **2008**, *33*, 1275–1285. [CrossRef]
27. Falsztinskij, W.S.; Diczkowski, R.E.; Łoziskij, W.G. Economical justification of effectiveness the sealing rockmass above the gas generator for borehole coal gasification. *Res. Rep. Min. Environ.* **2010**, *3*, 51–59. (In Polish)
28. Polish Standard: PN-EN 1936. *Natural Stone Research Methods—Determination of Density and Bulk Density as well as Total and Open Porosity*; Publishing Polish Committee for Standardization: Warszawa, Poland, 2010; pp. 1–12. (In Polish)
29. International Society for Rock Mechanics and Rock Engineering. Suggested Methods for Determining Tensile Strength of Rock Materials Part 2: Suggested Method for determining indirect tensile strength by the Brazil Test. *Int. J. Rock Mech. Min. Sci.* **1978**, *15*, 99–103. [CrossRef]
30. American Society of Testing and Materials. *Standard Test Method for Splitting Tensile Strength of Intact Rock Core Specimens*; ASTM D3967-16; ASTM International: West Conshohocken, PA, USA, 2016; pp. 1–5.
31. Rocscience. Available online: <https://www.rocscience.com> (accessed on 11 September 2021).
32. Białecka, B. Underground coal gasification. In *Basics of the Decision-Making Process*; Publishing House of the Central Mining Institute: Katowice, Poland, 2008; pp. 25–28. (In Polish)
33. Khan, M.M.; Mmbaga, J.P.; Shirazi, A.S.; Trivedi, J.; Liu, Q.; Gupta, R. Modelling Underground Coal Gasification—A Review. *Energies* **2015**, *8*, 12603–12668. [CrossRef]
34. Tian, H.; Kempka, T.; Schlüter, R.; Feinendegen, M.; Ziegler, M. Influence of high temperature on rock mass surrounding in situ coal conversion sites. In *Proceedings of the 10th International Symposium on Environmental Geotechnology and Sustainable Development*, Bochum, Germany, 7–11 September 2009; pp. 128–132.
35. Wolf, K.H.A.A.; Hettema, M.H.H.; Pater, C.J.; Van Hooydonk, R. Classification of overburden properties for underground coal gasification: Laboratory studies under high temperature and in situ stress conditions. In *Proceedings of the Rock Characterization: ISRM Symposium*, Eurock, Chester, UK, 14–17 September 1992; pp. 93–98.
36. Hettema, M.H.H.; Niepce, D.V.; Wolf, K.H.A.A. A microstructural analysis of the compaction of claystone aggregate at high temperature. *Int. J. Rock Mech. Min. Sci.* **1999**, *36*, 57–68. [CrossRef]
37. Wu, G.; Wang, Y.; Swift, G.; Chen, J. Laboratory investigation of the effect of temperature on the mechanical properties of sandstone. *Geotech. Geol. Eng.* **2013**, *31*, 809–816. [CrossRef]
38. Bresser, J.H.P.; Urai, J.L.; Olgaard, D.L. Effect of water on the strength and microstructure of Carrara marble axially compressed at high temperature. *J. Struct. Geol.* **2005**, *27*, 265–281. [CrossRef]
39. Luo, J.; Wang, L. High-temperature mechanical properties of mudstone in the process of underground coal gasification. *Rock Mech. Rock Eng.* **2011**, *44*, 749–754. [CrossRef]
40. Kiliç, Ö. The influence of high temperature on limestone P-wave velocity and Schmidt hammer strength. *Int. J. Rock Mech. Min. Sci.* **2006**, *43*, 980–986. [CrossRef]
41. Zhang, L.; Mao, X.; Lu, A. Experimental study on the mechanical properties of rocks at high temperature. *Sci. China Ser. E-Technol. Sci.* **2009**, *52*, 641–646. [CrossRef]
42. Rao, Q.-H.; Wang, Z.; Xie, H.-F.; Xie, Q. Experimental study of mechanical properties of sandstone at high temperature. *J. Cent. Univ. Technol.* **2007**, *14*, 478–483. [CrossRef]
43. Małkowski, P.; Skrzykowski, K.; Bożęcki, P. Changes of rock behaviour under the influence of high temperatures in the vicinity of a georeactor. *Res. Reports. Min. Environ.* **2011**, *4/2*, 259–272. (In Polish)

44. Otto, C.; Kempka, T. Thermo-mechanical simulations confirm: Temperature-dependent mudrock properties are nice to have in far-field environmental assessments of underground coal gasification. *Energy Procedia* **2015**, *76*, 582–591. [[CrossRef](#)]
45. Nakaten, N.; Kempka, T. Techno-Economic Comparison of Onshore and Offshore Underground Coal Gasification End-Product Competitiveness. *Energies* **2019**, *12*, 3252. [[CrossRef](#)]
46. Pivnyak, G.; Falshtynskiy, V.; Dychkovskiy, R.; Saik, P.; Lozynskiy, V.; Cabana, E.; Koshka, O. Conditions of Suitability of Coal Seams for Underground Coal Gasification. *Key Eng. Mater.* **2020**, *844*, 38–48. [[CrossRef](#)]
47. Dengina, N.I.; Kazak, V.N.; Pristash, V.V. Changes in rock at high temperature. *J. Min. Sci.* **1994**, *29*, 472–477. [[CrossRef](#)]
48. Luo, J.; Lianguo, W.; Furong, T.; Yan, H.; Lin, Z. Variation in the temperature field of rocks overlying a high-temperature cavity during underground coal gasification. *Min. Sci. Technol.* **2011**, *21*, 709–713. [[CrossRef](#)]
49. Wiatowski, M.; Kapusta, K.; Nowak, J.; Szyja, M.; Basa, W. An exsitu underground coal gasification experiment with a siderite interlayer: Course of the process, production gas, temperatures and energy efficiency. *Int. J. Coal. Sci. Technol* **2021**, *8*, 1–14. [[CrossRef](#)]
50. Xu, Y.; Li, H.; Guo, G.; Liu, X. Stability analysis of hyperbolic coal pillars with peeling and high temperature effects. *Energy Explor. Exploit.* **2020**, *38*, 1574–1588. [[CrossRef](#)]